

Fountain Sam (Orcid ID: 0000-0002-6028-0548)

Brock James (Orcid ID: 0000-0002-1381-1983)

Action of MK-7264 (Gefapixant) at human P2X3 and P2X2/3 receptors and *in vivo* efficacy in models of sensitisation

Richards, D¹., Gever, J.R²., Ford, A.P². and Fountain, S.J¹.

¹Biomedical Research Centre, School of Biological Sciences, University of East Anglia, Norwich Research Park, NR4 7TJ.

²Merck & Co., Inc., South San Francisco, CA 94080, USA

Running title: action of MK-7264 at P2X3 receptors

ABSTRACT

Background & purpose The P2X3 receptor is an ATP-gated ion channel expressed by sensory afferent neurons, and is as a target to treat chronic sensitisation conditions. The first-in-class, selective P2X3 and P2X2/3 receptor antagonist, the diaminopyrimidine MK-7264 (Gefapixant), has progressed to Phase III trials for refractory or unexplained chronic cough. We have used patch-clamp to elucidate the pharmacology and kinetics of MK-7264 and rat models of hypersensitivity and hyperalgesia to test efficacy in these conditions.

Experimental approach Whole-cell patch-clamp of 1321N1 cells expressing human P2X3 and P2X2/3 receptors was used to determine mode of MK-7264 action, potency and kinetics. The analgesic efficacy was assessed using paw withdrawal threshold and limb weight distribution in rat models of inflammatory, osteoarthritic and neuropathic sensitisation.

Key results MK-7264 is a reversible allosteric antagonist at human P2X3 and P2X2/3 receptors with IC₅₀ values of 153 and 220nM, respectively. Experiments with the slowly desensitising P2X2/3 heteromer revealed concentration and state-dependency to wash-on, with faster rates and greater inhibition when applied before agonist compared to during agonist application. Wash-on rate (τ value) for MK-7264 at maximal concentrations was 19s and 146s when applied before and during agonist application, respectively. *In vivo*, MK-7264 (30 mg/kg) displayed efficacy comparable to naproxen (20 mg/kg) in inflammatory and osteoarthritic sensitisation

This article has been accepted for publication and undergone full peer review but has not been through the copyediting, typesetting, pagination and proofreading process which may lead to differences between this version and the Version of Record. Please cite this article as doi: 10.1111/bph.14677

models, and gabapentin (100 mg/kg) in neuropathic sensitisation models, increasing paw withdrawal threshold and decreasing weight bearing discomfort.

Conclusions and implications MK-7264 is a reversible and selective P2X3 and P2X2/3 antagonist, exerting allosteric antagonism via preferential activity at closed channels. Efficacy in rat models supports clinical investigation of chronic sensitisation conditions.

ABBREVIATIONS ATP: adenosine 5'-triphosphate; α,β -meATP; α,β -methylene adenosine 5'-triphosphate

BULLET POINT SUMMARY

What is already known?

P2X3 is an ATP-gated ion channel expressed on sensory neurons. The antagonist MK-7264 has shown efficacy in a Phase 2b clinical trial for unexplained or refractory chronic cough.

What this study adds

This study reveals the mechanism of action of MK-7264 at human P2X3 and P2X2/3 receptors, and *in vivo* efficacy in pre-clinical models of sensitisation.

Clinical significance

MK-7264 has progressed to a Phase 3 trial for unexplained or refractory chronic cough, and has the potential to be clinically useful for conditions involving sensitisation.

INTRODUCTION

P2X receptors are a family of trimeric, ATP-gated ion channels (North, 2002). The human genome encodes seven pore-forming subunits (P2X1-7), that are capable of assembling as homomeric and heteromeric receptors in a subunit-dependent fashion (Surprenant & North, 2009). Each subunit has a double transmembrane topology and large extracellular domain which forms the orthosteric ATP binding site with an adjacent subunit (Kawate et al., 2009; Mansoor et al., 2016; Wang et al., 2018). Several P2X receptor subtypes are implicated in pain, irritation and hypersensitivity and have been proposed as drug targets, including the P2X3 receptor and P2X2/3 heteromeric receptor (Jarvis et al., 2002; Gevers et al., 2010; Pijacka et al., 2016; Stokes et al., 2017). P2X3 receptor tissue expression is very limited with protein and mRNA transcript detected in small diameter C-fiber sensory neurons (Chen et al., 1995; Lewis et al., 1995; Xiang et al., 1998), particularly those innervating the skin and viscera (Bradbury et al., 1998), petrosal neurons and the carotid body afferents (Pijacka et al., 2016). P2X3 and P2X2/P2X3 double knockout mice display reduced nocifensive responses to ATP and formalin injection, as well as bladder hyporeflexia (Cockayne et al., 2000; Cockayne et al., 2005), and both dorsal root and nodose ganglia neurons lose sensitivity to the selective agonist α,β -meATP (Zhong et al., 2001). P2X3 expression increases in rat models of inferior alveolar nerve injury (Eriksson et al., 1998), complete Freund's adjuvant-induced monoarthritis (Shinoda et al., 2005) and cast immobilisation (Sekino et al., 2014). In rat models, the number of P2X3-positive small diameter L4 and L5 dorsal root ganglion neurons increases after chronic constriction of the sciatic nerve (Novakovic et al., 1999) but decreases following axotomy (Bradbury et al., 1998). In humans, P2X3 expression is increased in bladder urothelium during interstitial cystitis (Tempest et al., 2004), endometriosis endometrium and endometriosis lesions (Ding et al., 2017).

Studies in knockout mice (Cockayne et al., 2000; Cockayne et al., 2005) as well as RNAi (Barclay et al., 2002; Honore et al., 2002), small molecule antagonists (Jarvis et al., 2002; McGaraughty et al., 2003; Kaan et al., 2010), the spider venom peptide purotoxin-1 (Grishin et al., 2010) and blocking monoclonal antibodies (Shcherbatko et al., 2016) have all demonstrated the efficacy of P2X3 and P2X2/3 antagonism to reduce nocifensive responses, and neuropathic, inflammatory, arthritic and visceral pain. Such studies validate P2X3 as a therapeutic target for chronic sensitisation conditions.

P2X3 and P2X2/3 receptors are antagonised by a range of molecules with poor selectivity and potency, including suramin, pyridoxal phosphate-6-azo (benzene-2,4-disulphonic acid) (PPADS) and reactive blue 2, in addition to 2',3'-O-(2,4,6-trinitrophenyl) ATP (TNP-ATP) which has low metabolic stability (North, 2002). Such molecules are therefore compromised for *in vivo* investigation (Jarvis et al., 2001; Ueno et al., 2003). A-317491 (Jarvis et al., 2002), a more potent and selective P2X3 and P2X2/3 antagonist has been developed, however this molecule suffers from several undesirable characteristics including low oral bioavailability and very high protein binding (>99.9%). MK-7264 (formerly AF-219) is diaminopyrimidine antagonist of human P2X3 and P2X2/3 receptors. The compound has reached Phase 2 proof of concept trials for pain in osteoarthritis of the knee and interstitial cystitis/bladder pain (Ford and Undhem, 2013) and Phase 2b trials for refractory chronic cough (Abdulqawi et al., 2015) whereby daytime cough frequency was significantly reduced compared to placebo. MK-7264 is the first-in-class selective P2X3 antagonist, named Gefapixant, and has progressed to a Phase 3 trial for unexplained or refractory chronic cough (NCT03449134). This drug is peripherally restricted but the close structural analogue, AF-353 is able to traverse the blood-brain barrier (Gever et al., 2010). Though the mechanisms underlying chronic cough are not fully understood, it is widely accepted that heightened sensitivity of afferent limb of the cough reflex plays an important role in the disease (Higenbottam, 2002). The efficacy of P2X3 antagonists as anti-tussive agents in humans is likely due to the blockade of P2X3 receptors expressed on the sensory neurons within the afferent limb of the cough reflex (Ford, 2012). Mice and rats lack a cough reflex and are therefore not useful in studying the efficacy of P2X3 antagonists as anti-tussive agents *in vivo* (Mazzone, 2005). However, these preclinical models are useful in studying the *in vivo* effects of P2X3 receptor in other processes that involve afferent sensitisation and hyperalgesia. Here we electrophysiologically characterise MK-7264 at human P2X3 and P2X2/3 receptors and determine *in vivo* efficacy in rat models of sensitisation.

MATERIALS AND METHODS

Study ethics

All animal experiments were performed at Pharmaron (Beijing, China). Experiments were performed according to the guidelines approved by the Institutional Animal Care and Use Committee (IACUC) of Pharmaron following the guidance of the Association for Assessment and Accreditation of Laboratory Animal Care International (AAALAC).

Drugs and salts

All basic salts, ATP, sodium carboxymethyl cellulose, gabapentin, naproxen and mono-iodoacetic acid were purchased from Sigma. Complete Freund's adjuvant was purchased from Chondrex. α,β -meATP was purchased from Tocris. For electrophysiological studies, all drugs were dissolved in DMSO, with the final DMSO concentration of 0.1% (v/v) in all experiments. For *in vivo* studies, all drugs were dissolved in 0.5% (w/v) sodium carboxymethyl cellulose and administered orally at a volume of 5mL/kg.

Cells

1321N1 astrocytoma lines (RRID:CVCL_0110) stably transfected with human P2X2, P2X3 or co-expressing P2X2 and P2X3 receptors were used in all experiments, and provided by Afferent Pharmaceuticals Ltd. Cells were cultured in Dulbecco's Modified Eagle's Medium with 4.5g/L glucose, 4mM L-glutamine, 50 IU/mL penicillin, 50 μ g/mL streptomycin and 10% (v/v) FBS. Cells were cultured in the presence of either G418 (P2X2), puromycin (P2X3) or G418 plus puromycin (P2X2/3) selection antibiotics. Cells were maintained at 37°C and 5% CO₂.

Patch-clamp electrophysiology

Cells were resuspended at 1×10^6 cells/mL in solution containing (mM): NaCl, 140; KCl, 4mM; MgCl₂, 1; CaCl₂, 2; D-glucose, 5 and HEPES, 10; pH7.4). Whole-cell planar patch-clamp was conducted using a Nanion port-a-patch system fitted with an 8-valve gravity fed perfusion panel. The time for total solution exchange was <150ms. Internal solution contained (mM): CsF, 120; NaCl, 10; MgCl₂, 2; HEPES, 10; pH7.2. Following gigaseal formation, all recordings were performed in external solution containing (mM): NaCl, 155; KCl, 3; MgCl₂, 1; CaCl₂, 1.5; HEPES, 10; pH7.4. Acquisition protocols were run using HEKA Patchmaster software (RRID: SCR_000034) and a HEKA EPC 10 amplifier. Data was sampled at 1 kHz and filtered at 10 kHz. Cells were held at -80mV in all experiments. All recordings were performed at room temperature (21 – 23°C). Tau values (τ) were calculated by fitting a single exponential decay curve to the desensitisation phase of current traces using Origin Pro software (version 2016; Originlab).

Animals

5-7 week old female Sprague-Dawley rats (150-180g) (RRID:RGID_10395233) were obtained from the Beijing Vital River Company. Animals were housed at 22 (\pm 3°C) with 12 hours of fluorescent lighting per day and food and water available *ad libitum*. Animals were kept for one week prior to the start of experiments, health checked and randomly assigned to groups. Experiments began when animals were 6-8 weeks old (180-220g). MK-7264, naproxen and gabapentin were dissolved in 0.5% (w/v) sodium carboxymethyl cellulose (Sigma) and administered by oral gavage at 5mL/kg.

Complete Freund's Adjuvant (CFA) inflammatory hyperalgesia

The CFA model of inflammation leads to edema as well as mechanical allodynia of the injected paw (Stein et al., 1988). 50 μ L of CFA (Chondrex) was injected into left hind paw subplantar 7 days prior to experimentation.

Mono-iodoacetate (MIA) induced osteoarthritis

Mono-iodoacetic acid is an inhibitor of glyceraldehyde-3-phosphate dehydrogenase causing the death of chondrocytes, and histological and pathophysiological changes observed in osteoarthritis (Bove et al., 2003). 50 μ L of 0.9% normal saline containing 3mg MIA (Sigma) was injected through the patellar ligament into the right hind knee. The injection was conducted under isoflurane anaesthesia 13 days prior to experimentation.

Spared nerve injury (SNI) neuropathic pain model

The spared nerve injury model induces increased mechanical and thermal sensitivity of the treated paw, mimicking clinical neuropathic pain (Decosterd & Woolf, 2000). The sciatic nerve and its three terminal branches (sural, common peroneal and tibial nerves) were exposed by skin incision on the lateral surface of the thigh and by sectioning the biceps femoris muscle of the left lateral leg. The peroneal and tibial nerve were ligated and 4 \pm 2 mm of the distal nerve stump was axotomized followed by muscle and skin closure. The sural nerve was not ligated and remained intact. Surgery was conducted under anaesthesia 10 days prior to

experimentation. Anaesthesia was induced using 5% isoflurane and maintained at 3% isoflurane with a gas flow of 1L/min using a precision vaporizer. The level of anaesthesia was monitored by heart rate, respiratory rate, temperature and pedal reflex. Animals received post-operative analgesia via subcutaneous injection of carprofen (5mg/kg) for up to 72 hours. For sham animals, the sciatic nerve was exposed via a skin incision on the lateral surface of the thigh followed by sectioning of the biceps femoris muscle, but the nerve was not axotomized. Post-operative analgesia was provide for sham animals as for animals undergoing sciatic nerve axotomy.

Von Frey filaments testing for mechanical allodynia

The paw withdrawal threshold was measured by applying Von Frey filaments (Bioseb) of increasing force, perpendicularly to the plantar surface of the hind paw of the treated limb. Following acclimatisation, rats were allowed to stand on mesh and filaments were applied from beneath. The average of 2-3 repeated stimuli was taken as the withdrawal threshold. Experimenters were blinded to drug treatments.

Static weight bearing test for joint discomfort

Weight redistribution between hind paws was measured using a weight balance changing instrument (Bio-medical, USA). Weight distribution (g) is calculated as contralateral limb minus ipsilateral limb weight bearing, hence the difference diminishes as hyperalgesia is reduced. Average weight bearing was measured over a 10 s period. Experimenters were blinded to drug treatments.

Pharmacokinetic profiling

Rats received a single oral dose of MK-7264 and a single blood sample was taken from each animal by the retro-orbital route for a given time point. Retro-orbital sampling was performed under general anaesthesia. General anaesthesia was induced by intraperitoneal injection of ketamine (80 mg/kg) and xylazine (10 mg/kg). The level of anaesthesia was monitored by heart rate, respiratory rate, temperature and pedal reflex. Following blood sampling, animals were not recovered from general anaesthesia and sacrificed by CO₂ asphyxiation. MK-7264

quantification was determined by liquid chromatography-tandem mass spectrometry (API 4000 QTrap, Applied Biosystems).

Data and statistical analysis

All statistical analysis was performed using Origin Pro (version 2016; Originlab), unless otherwise stated. The threshold for statistical significance was $P < 0.05$ throughout. Data was first tested with a Shapiro-Wilk test for normality and Levene's test for equality of variance. For antagonist IC_{50} datasets, the normalised response was plotted against Log_{10} antagonist concentration and fitted with a modified Hill Equation as below:

$$Y = \text{Start} + (\text{End} - \text{Start}) \frac{X^n}{k^n + X^n}$$

Where k = Michealis constant and n = number of cooperative sites. The datasets were then compared with an F-test. Pairwise comparison of EC_{50} values generated in curve shift experiments was conducted using a paired sample T-test. Wash-on rate in the presence and absence of agonist was compared with a One-way ANOVA followed by Tukey post-hoc test. τ_{on} and τ_{off} rates were estimated by fitting a single exponential decay curve to the desensitisation phase of current traces:

$$Y = A \times \exp\left(\frac{-x}{t}\right) + Y_0$$

Where Y_0 = offset, A = amplitude and t = time constant. τ of desensitisation and residual current data was compared with a Kruskal-Wallis ANOVA followed by Dunn's post hoc test. Analyses of paw withdrawal (Von Frey filaments) and static weight bearing were conducted with a two-way repeated measures ANOVA. The two factors were (A) time of measurement after drug treatment (within groups measure) and (B) drug treatment (between groups measure). Where significant interactions were detected, a subsequent Fisher least significant difference post-hoc test was used to compare the effect of drug treatments at individual time points.

Nomenclature of Targets and Ligands

Key protein targets and ligands in this article are hyperlinked to corresponding entries in <http://www.guidetopharmacology.org>, the common portal for data from the IUPHAR/BPS Guide to PHARMACOLOGY (Harding *et al.*, 2018), and are permanently archived in the Concise Guide to PHARMACOLOGY 2017/18 (Alexander *et al.*, 2017).

RESULTS

MK-7264 antagonises P2X3-containing receptors selectively and reversibly

Human P2X3 expressed in 1321N1 cells displayed rapidly desensitising (millisecond) agonist evoked inward currents that recover slowly (**Figure 1A**). Complete recovery for responses to α,β -meATP was achieved using an interval of 4 minutes between agonist application (**Figure 1A**). P2X2/3 mediated currents were isolated in 1321N1 co-expressing P2X2 and P2X3 by using α,β -meATP which does not activate P2X2 homomers. In some cells, initial responses in 1321N1 co-expressing P2X2 and P2X3 to α,β -meATP evoked mixed P2X3 (transient, rapidly desensitising) and P2X2/3 (slowly desensitising) responses, however the contribution of P2X3 homomer responses was lost after several α,β -meATP applications at 30s intervals leaving P2X2/3 currents for further investigation (**Figure 1B**). MK-7264 could potentially inhibit P2X3 and P2X2/3 currents in a reversible and concentration-dependent fashion (**Figures 1A and 1B**). No effect of 10 μ M MK-7264 on human P2X2 currents was observed ($N=5$) (**Figure 1C**). The half-maximal concentration of MK-7264 antagonism at P2X3 and P2X2/3 receptors was 153 ± 59 nM ($N=5$) and 220 ± 47 nM ($N=5$) (**Figure 1D**), respectively. These were found to be significantly different by an F-test ($F = 11.74$, $p < 0.05$). Measurements were made for reduction in peak and steady-state currents for P2X3 and P2X2/3 respectively. The Hill coefficient for MK-7264 concentration inhibition was 1.0 ± 0.4 for P2X3 and 1.0 ± 0.2 for P2X2/3, indicating MK-7264 acts in a non-cooperative manner. Antagonism of human P2X3 receptors using a submaximal MK-7264 concentration (300nM; approximate IC_{70}) was not surmounted by increasing the concentration of α,β -meATP agonist (**Figure 1E**), indicating MK-7264 acts independently of agonist concentration to block P2X3. In addition to suppression of response maxima, MK-7264 also significantly reduced α,β -meATP potency (EC_{50} $1.0\pm 0.1\mu$ M vehicle *versus* $6.0\pm 1.5\mu$ M with 300nM MK-7264; $N=5$, paired sample T-test

$p < 0.05$). These data suggest MK-7264 is a negative allosteric modulator of the human P2X3 receptor.

Onset and offset of MK-7264 action

Due to the prolonged recovery time required and rapid intrinsic desensitisation of P2X3 receptors, the slowly desensitising and rapidly recovering P2X2/3 receptor was used to quantify wash-on and wash-off rates of MK-7264. Agonist applied for 2s every 30s allowed for complete recovery of the P2X2/3 response, we therefore applied α, β -meATP every 30s whilst bath perfusing a maximal concentration of MK-7264 until steady-state inhibition of the P2X2/3 current was achieved (**Figure 2A and 2B**). To quantify wash-off, vehicle was bath perfused following a period of steady-state inhibition and recovery monitored by agonist application every 30s until steady-state response were obtained (**Figure 2B**). For all wash-on and wash-off experiments, the mean current (1-2 s from onset) was then normalised against the vehicle control response. Exponential decay curves were fitted to individual data sets and τ_{on} and τ_{off} derived from curve time constants (**Figure 2B**). The concentration-dependency of MK-7264 τ_{on} and τ_{off} are given in **Table 1**. The τ_{on} rate decreased with increasing concentrations of MK-7264 ranging between 12 – 360s for the concentration range 100nM – 3 μ M. The τ_{off} value increased with decreasing concentrations of MK-7264.

MK-7264 action before and during agonist application

The slow intrinsic desensitising properties of P2X2/3 currents provided the opportunity to investigate the effects of rapid MK-7264 application to activated channels. In these experiments, currents were initiated by rapid 2s perfusion of α, β -meATP, quickly followed by combined rapid perfusion of α, β -meATP and MK-7264 allowing the effect of MK-7264 on the steady-state current to be quantified (**Figure 2C**). The current magnitude was quantified every 5s following MK-7264 co-application. We observed that the on rate of inhibition by MK-7264 was significantly greater following application to the closed versus open channel (**Figure 2D**), with MK-7264 inhibiting the response by $83 \pm 2\%$ compared to $41 \pm 5\%$ following a 30s perfusion prior to agonist application and during agonist application, respectively (One-way ANOVA $F = 45.94$, $p = < 0.05$, followed by Tukey post hoc test) (**Figure 2A vs Figure 2D**).

Changes in P2X3 receptor desensitisation

MK-7264 antagonism of human P2X3 was associated with a slowing of the second phase of desensitisation that was relieved upon agonist wash-off (**Figure 3A**). This apparent slowing of desensitisation kinetic of the response was different from control response which decayed to baseline during agonist application (**Figure 3A**). The desensitisation phase of P2X3 after MK-7264 exposure consists of a rapid phase (~200ms) which is characteristic of P2X3 and appears unchanged apart from the reduction in magnitude, followed by a slower phase with shallow gradient dependent upon MK-7264 concentration. This prolonged desensitisation effect of MK-7264 washed-off at a similar rate to the inhibition of peak response (**Figure 3B**). The prolonged desensitisation phase is shallow and not well fit by a single exponential curve to calculate a τ value, and therefore a curve was fitted 250-750ms after the onset of agonist response to estimate the rate of this phase (**Figure 3A** and **3C**). MK-7264 at 1 μ M significantly decreased the rate of desensitisation from 206 ± 11 ms to 6.6 ± 3.5 s ($N=6$; Kruskal-Wallis ANOVA followed by Dunn's post hoc $p < 0.05$ versus vehicle control), respectively. The residual current at one second after onset of agonist response was measured and shown as a fraction of peak current in Figure 3D. The residual current increased with antagonist concentration and was significantly different from the vehicle control at 300 nM and 1 μ M (Kruskal-Wallis ANOVA followed by Dunn's post hoc test, $p < 0.05$).

Efficacy of MK-7264 in rat model of inflammatory hyperalgesia

MK-7264 and the non-steroidal anti-inflammatory naproxen were tested for their ability to reduce mechanical sensitivity and weight-bearing discomfort in a Complete Freund's Adjuvant (CFA) model of inflammatory hyperalgesia (**Figure 4**). For the Von Frey measurements there was significant differences between the time of measurement ($F = 17.6$, $p < 0.05$), the treatments ($F = 24.4$, $p < 0.05$) and the interaction between these factors ($F = 5.03$, $p < 0.05$). For weight bearing measurements there were significant differences between the time of measurement ($F = 44.29$, $p < 0.05$), the treatments ($F = 28.8$, $p < 0.05$) and the interaction between these factors ($F = 9.97$, $p < 0.05$). Fisher least significant difference post hoc test indicated that both naproxen and MK-7264 at 20 mg/kg and 30 mg/kg respectively, significantly reduced mechanical sensitivity (increased paw-withdrawal) threshold compared to vehicle control, 1 and 3 hours after dosing and to a comparable level ($N=10$; $p < 0.05$ for both

treatments versus vehicle control) (**Figure 4A**). The maximum reduction for both treatments was observed at 3 hours, where the mean withdrawal threshold was $6.0\pm 0.6\text{g}$, $8.2\pm 0.9\text{g}$ and $8.1\pm 0.5\text{g}$ for vehicle, naproxen and MK-7264, respectively. Withdrawal threshold was $13.3\pm 0.2\text{g}$ ($N=20$) in naïve control animals. MK-7264 was also efficacious in reducing weight-bearing discomfort at 1 and 3 hours after dosing (**Figure 4B**). The maximum effect of MK-7264 (30 mg/kg) was observed at 3 hours and similar to that of naproxen (20 mg/kg), where difference in weight bearing between contralateral and ipsilateral limbs was $55\pm 6\text{g}$, $35\pm 4\text{g}$ and $34\pm 4\text{g}$ for vehicle control, MK-7264 and naproxen ($N=10$; $p<0.05$ for all treatments versus vehicle control), respectively. These values are compared to $5.8\pm 0.8\text{g}$ ($N=12$) for sham animals. Individual differences detected with a Fisher least significant difference post-hoc test are shown in Figure 4.

Efficacy of MK-7264 in rat model of osteoarthritis pain

MK-7264 *in vivo* efficacy was investigated further to provide relief from mechanical hypersensitivity in a model of monoiodoacetate (MIA)-induced osteoarthritis. In these experiments three doses of MK-7264 (3, 10 and 30 mg/kg) were compared with naproxen (20 mg/kg) and vehicle control (**Figure 5A**). For the Von Frey measurements there were significant differences between the time of measurement ($F = 157.27$, $p < 0.05$), the treatments ($F = 87.99$, $p < 0.05$) and the interaction between these factors ($F = 30.37$, $p < 0.05$). For weight bearing measurements there were significant differences between the time of measurement ($F = 44.8$, $p < 0.05$), the treatments ($F = 14.35$, $p < 0.05$) and the interaction between these factors ($F = 4.96$, $p < 0.05$). A Fisher least significant difference post hoc test indicated that naproxen and MK-7264 at 10 and 30 mg/kg significantly increased the paw-withdrawal threshold 1 and 3 hours after administration (**Figure 5A**). The maximum effect of all drug treatments was observed at 3 hours following administration, where the paw-withdrawal threshold for $6.4\pm 0.7\text{g}$, $10.9\pm 0.6\text{g}$, $9.6\pm 0.8\text{g}$ and $10.7\pm 0.8\text{g}$ for vehicle control, naproxen, and MK-7264 at 10 mg/kg and 30 mg/kg, respectively ($N=10$; $p<0.05$ for all treatments versus vehicle control). Withdrawal threshold was $13.3\pm 0.2\text{g}$ ($N=20$) in control animals. MK-7264 at 3 mg/kg produced no significant effect over vehicle control (**Figure 5A**). Similar effects of MK-7264 dosing were observed in reducing the difference in weight bearing between contralateral and ipsilateral limbs in the osteoarthritis model at 1 and 3 hours following administration (**Figure 5B**). Naproxen and MK-7264 (30 mg/kg) significantly reduced the difference in weight bearing

between contralateral and ipsilateral limbs to 24.2 ± 4.1 g and 24.5 ± 3.1 g, respectively, compared to 35.9 ± 4.1 g in vehicle control ($N=10$; $p < 0.05$ for treatments versus vehicle control). These values are compared to 6.8 ± 0.5 g ($N=10$) for sham animals. Individual differences detected with a Fisher least significant difference post-hoc test are shown in Figure 5.

Efficacy of MK-7264 in rat neuropathic pain model

Finally we sought further verification for the *in vivo* efficacy of MK-7264 in a rat model of neuropathic pain (**Figure 6**). Hypersensitivity was assayed by measurement of paw-withdrawal threshold and weight-bearing discomfort. In a Phase I experiment to determine the efficacy of MK-7264 in reducing hypersensitivity, animals were administered with either vehicle control, gabapentin (100mg/kg) as a positive control, or MK-7264 at either 10 or 30 mg/kg. Paw-withdrawal threshold and weight-bearing discomfort were measured 1, 3 and 8 hours following administration. For Von Frey assessment of paw-withdrawal threshold, there were significant differences between the time of measurement ($F = 22.99$, $p < 0.05$), the treatments ($F = 11.75$, $p < 0.05$) and the interaction between these factors ($F = 2.18$, $p < 0.05$) (**Figure 6A**). Nerve injury produced hypersensitivity as assessed by paw-withdrawal. Thresholds were 7.4 ± 0.5 g ($N=10$) for animals that underwent nerve injury, compared to 13.3 ± 0.2 g ($N=20$; $p < 0.05$) for sham surgery animals. Gabapentin (100 mg/kg), and MK-7264 administered at 10 mg/kg and 20 mg/kg all significantly increased paw-withdrawal threshold compared to vehicle control at 1 and 3 hours post administration (**Figure 6A**). Following phase I experiments, a second dosing regimen was undertaken to test for drug tolerance. In these experiments (termed phase II), animals were repeatedly dosed for 12 hour intervals and drug efficacy re-evaluated at the same timepoints as phase I starting at day 5.5. For the Von Frey measurements there were significant differences between the time of measurement ($F = 22.13$, $p < 0.05$), the treatments ($F = 49.61$, $p < 0.05$), and the interaction between these factors ($F = 6.57$, $p < 0.05$). After the 5.5 day repetitive dosing regimen, administration of gabapentin (100 mg/kg) and MK-7264 (30 mg/kg) significantly increased paw-withdrawal threshold for 8 hours post administration compared to administration of vehicle control (**Figure 6B**). The efficacy of MK-7264 at 10 mg/kg diminished significantly after 3 hours post administration (**Figure 6B**).

For Phase I weight-bearing discomfort measurements, there were significant differences between the time of measurement ($F = 25.64$, $p < 0.05$) and the treatments ($F = 14.35$, $p < 0.05$), but no significant interaction between these factors (**Figure 6C**). Nerve injury produced hypersensitivity as assessed by weight-bearing discomfort. Difference in weight bearing between contralateral and ipsilateral limbs were $51.1 \pm 7.8\text{g}$ ($N=10$) for animals that underwent nerve injury, compared to $5.8 \pm 0.8\text{g}$ ($N=12$; $p < 0.05$) for sham surgery animals. In Phase I experiments, administration of gabapentin (100 mg/kg) or MK-7264 at 10 mg/kg and 30 mg/kg significantly reduced the difference in weight bearing between contralateral and ipsilateral limbs up to 3 hours post administration compared to administration of vehicle control (**Figure 6C**). In phase II experiments of weight-bearing discomfort, there were significant differences between the time of measurement ($F = 4.21$, $p < 0.05$) and drug treatment ($F = 12.68$, $p < 0.05$). Administration of gabapentin (100 mg/kg) and MK-7264 at 30 mg/kg caused a significant reduction in the difference in weight bearing between contralateral and ipsilateral limbs up to 3 hours post administration compared to administration of vehicle control (**Figure 6D**). MK-7264 at 10 mg/kg reduced weight-bearing difference up to 1 hour but its effects had diminished by 3 hours (**Figure 6D**).

MK-7264 blood plasma concentration following dosing in vivo in rats

Rats received a single oral doses of MK-7264 and plasma concentrations were determined for different dosages at 0, 1 and 3 hours after dosing to determine the pharmacokinetic profile (Figure 7). The plasma concentration following a single oral dose of MK-7264 was determined post administration by orbital blood sampling to correlate with exposure times that proved efficacious in inflammatory pain models. After 3 hours, plasma concentrations ranged from 250 – 1087nM (mean $605 \pm 257\text{nM}$; $N=10$) for 10 mg/kg, 365 – 1882nM (mean $1027 \pm 597\text{nM}$; $N=10$) for 20 mg/kg, and 1194 – 3396nM (mean $2077 \pm 775\text{nM}$; $N=10$) for 60 mg/kg.

DISCUSSION

These studies reveal nanomolar potency of the human P2X3 and P2X2/3 receptor antagonist MK-7264, with marginal selectivity for P2X3 over recombinant P2X2/3 receptors. Both P2X3 and P2X2/3 are expressed by somatosensory neurons (Chen et al., 1995; Lewis et al., 1995; Bradbury et al., 1998), and selective antagonism of these receptors reduces nocifensive

responses in several rat models of pain (Jarvis et al., 2002; McGaraughty et al., 2003; Kaan et al., 2010; Grishin et al., 2010). Our pharmacological analysis demonstrates that the action of MK-7264 is insurmountable by increasing agonist concentration. Like its structural relative AF-353 (Gever et al., 2010), MK-7264 attenuated the response maxima in addition to decreasing agonist potency. This demonstrates that MK-7264 does not act as a pure non-competitive antagonist, but rather exerts its antagonism through negative allosteric modulation of the P2X3 receptor. The allosteric nature of MK-7264 is supported by the recent publication of the human P2X3 homomeric receptor with MK-7264 bound (Wang et al., 2018). Radioligand binding studies with AF-353 (Gever et al., 2010) suggest that this series of compounds does not alter agonist affinity but rather negatively modulates efficacy. The proposed MK-7264 binding site resides within an inter-subunit interface created by the lower body and dorsal fin of one P2X3 subunit and the lower body domain of an adjacent P2X3 subunit. This site is distinct from the orthosteric ATP binding site in P2X receptors (Mansoor et al., 2016) and supportive of MK-7264 acting allosterically. Interestingly, the key residues proposed to form the MK-7264 binding site by Wang et al (2018) have a high degree of physicochemical conservation across all human P2X receptors. Our observation that human P2X2 homomeric receptors are insensitive to MK-7264 suggests that the presence of these residues alone is not sufficient to convey sensitivity, rather the spatial positioning of these residues is important. This hypothesis is supported by *in silico* measurements of the spatial distribution of these key residues indicates that they are spaced further apart in the zebrafish P2X4 crystal structure (Kawate et al., 2009), which mostly shares the key MK-7264 binding residues with human P2X3 but they are spatially further apart. The stoichiometry of native P2X2/3 remains undetermined, but at least one P2X3-P2X3 interface may exist and convey MK-7264 sensitivity to the P2X2/3 heteromer, though with slightly less sensitivity compared to P2X3 homomeric receptors. It is also possible that a P2X2-P2X3 interface creates a suitable binding pocket.

The wash-on rate of MK-7264 to the P2X2/3 receptor was concentration-dependent and significantly attenuated in the presence of agonist, and as with AF-353, the high compound potency is due to comparatively slow on and off rates (Gever et al., 2010). This is in contrast to rapid rates of other P2X receptor antagonists such as PPADS (Li, 2000), TNP-ATP and suramin (Spelta et al., 2002). The disparity in MK-7264 wash-on rate in the absence (presumed predominantly closed channel population) and presence (presumed predominantly open/desensitising channel population) indicates that MK-7264 exerts its effects more rapidly

at agonist unbound (closed) channels. This is in contrast to PPADS which was found to bind three times more rapidly to the open over the closed P2X_{2/3} receptor (Spelta et al., 2002). The crystal structure of human P2X₃ in the open and closed conformation (Mansoor et al., 2016) indicates that the MK-7264 binding pocket undergoes a dynamic change upon ATP binding, whereby the dorsal fin domain shifts upwards and the left fin moves downwards. This structural transition disrupts the MK-7264 binding pocket and is the likely molecular basis for the disparity between MK-7264 on-rates in the presence and absence of agonist. A further pharmacological characteristic of MK-7264 is a slowing of the rate of desensitisation. The reason for this slowing of desensitisation and propagation of a residual current is not known, but it could be that MK-7264 binding interferes with the transition of open to desensitised channel. An alternative explanation may be that partial antagonist saturation of the receptor leads to a non-desensitising conductance or sub-conductance state. The observation that this effect is relieved upon agonist wash-off indicates that it is an agonist-dependent process. Although mechanistically interesting, this slowing of desensitisation observed under conditions of voltage-clamp does not prevent the therapeutic activity of MK-7264 in humans (Abdulgawi et al., 2015) or in rat models. MK-7264 has a relatively slow time course of action in the *in vivo* rat models employed in this study. The slow on/off rates at the receptor level cannot completely account for this observation. The pharmacokinetics of MK-7264 following oral dosing are likely to be a major contributor to the slow onset of *in vivo* efficacy. A sufficiently high concentration of MK-7264 to achieve complete blockade of P2X₃ (low micromolar) is achieved by 1 hour in doses in excess of 20 mg/kg (but not at 10 mg/kg) and maintained until at least 3 hours. The time taken for plasma concentrations to peak to a point where P2X₃ receptors are maximally blocked in *in vitro* experiments is likely to account for why the greatest *in vivo* efficacy is not observed until 3 hours after dosing.

ATP is released by mammalian cells under inflammatory conditions, both passively from cells undergoing lysis, and actively via vesicular and channel mediated processes (Dosch et al., 2018). The expression of P2X₃ on somatosensory neurons therefore makes it a potential target for a range of peripheral sensory disorders (Ford, 2012). In both the Complete Freund's adjuvant model of inflammatory hyperalgesia and the monosodium iodoacetate injection model of osteoarthritis, 30 mg/kg MK-7264 acted with the same efficacy as 20 mg/kg naproxen, indicating MK-7264 provides relief from inflammatory and osteoarthritic pain in these models. In the spared nerve injury model of neuropathic pain, acute MK-7264 dosing could relieve pain with the same efficacy as 100 mg/kg gabapentin. After chronic dosing with MK-7264, the

response to acute noxious stimuli (Von Frey) was reduced at all time points tested, but this did not translate to a prolonged reduction in weight bearing discomfort. These data indicate that MK-7264 works efficaciously to reduce pain hypersensitivity *in vivo*. MK-7264 was as effective as current treatments and continued to show efficacy after repeated dosing in the neuropathic pain model, suggesting lack of tolerance. Finally, the plasma concentrations of MK-7264 at 3 hours post oral administration suggest high bioavailability, with low micromolar plasma concentrations achieved at 20 and 60 mg/kg. These concentrations are sufficient to reduce P2X3 and P2X2/3 activity by 75-95% *in vitro* and significantly reduce rat nocifensive responses and discomfort *in vivo*. MK-7264 is peripherally restricted (Pijacka et al., 2016) and therefore the *in vivo* effects are not the result of centrally mediated mechanisms. ATP released from damaged or inflamed tissues can activate P2X receptors expressed on primary afferent neurons. The resulting depolarization can initiate action potentials that are interpreted centrally as pain (North, 2004). This is also observed in humans where intracutaneous injections of ATP elicited discharge of afferent neurons innervating the peroneal nerve (Hilliges et al., 2002). P2X3 has very limited expression, predominantly located on afferent neurons, including those innervating the skin, viscera, and knee joint (Bradbury et al., 1998; Teixeira et al., 2017). Inhibition of P2X3-dependent action potential of afferent neurons innervating peripheral tissue and nerves is therefore the likely mechanism mediating the *in vivo* effects of MK-7264 in pain models.

In summary, MK-7264 is a first-in-class, selective, reversible and orally bioavailable P2X3 and P2X2/3 receptor antagonist with *in vivo* efficacy for the relief of inflammatory, osteoarthritic and neuropathic pain. MK-7264 likely exerts its antagonism via negative allosteric modulation.

ACKNOWLEDGEMENTS

This work was funded by Afferent Pharmaceuticals and Merck Sharp & Dohme Corp., a subsidiary of Merck & Co., Inc., Kenilworth, NJ, USA.

AUTHOR CONTRIBUTIONS

DR undertook the experimental work, analysis and manuscript writing. APF undertook experimental analysis and study design. JRG and SJF undertook data analysis, study design and wrote the manuscript.

CONFLICT OF INTEREST

Authors declare no conflict of interest.

DECLARATION OF TRANSPARENCY AND SCIENTIFIC RIGOUR

This Declaration acknowledges that this paper adheres to the principles for transparent reporting and scientific rigour of preclinical research as stated in the *BJP* guidelines for Design & Analysis, and Animal Experimentation, and as recommended by funding agencies, publishers and other organisations engaged with supporting research.

REFERENCES

- Abdulqawi, R., Dockry, R., Holt, K., Layton, G., McCarthy, B.G., Ford, A.P et al. (2015). “P2X3 receptor antagonist (AF-219) in refractory chronic cough: a randomised, double-blind, placebo-controlled phase 2 study”. *The Lancet*. **28** (385): 1198-1205.
- Alexander, SPH, Christopoulos, A, Davenport, AP, Kelly, E, Marrion, NV, Peters, JA *et al.* (2017a). The Concise Guide to PHARMACOLOGY 2017/18: G protein-coupled receptors. *Br J Pharmacol* **174**: S17– S129.
- Barclay, J., Patel, S., Dorn, G., Wotherspoon, G., Moffatt, S., Eunson, L. et al. (2002). “Functional downregulation of P2X3 receptor subunit in rat sensory neurons reveals a significant role in chronic neuropathic and inflammatory pain”. *Journal of Neuroscience*. **22** (18): 8139-8147.
- Bove, S.E., Calcaterra, S.L., Brooker, R.M., Huber, C.M., Guzman, R.E., Juneau, P.L et al. (2003). “Weight bearing as a measure of disease progression and efficacy of anti-inflammatory compounds in a model of monosodium iodoacetate-induced osteoarthritis”. *Osteoarthritis and Cartilage*. **11**: 821-830.
- Bradbury, E.J., Burnstock, G. & McMahon, S.B. (1998). “The expression of P2X3 purinoreceptors in sensory neurons: Effects of axotomy and glial-derived neurotrophic factor”. *Molecular and Cellular Neuroscience*. **12** (4-5): 256-268.
- Chen, C., Akopjan, A.N., Sivilotti, L. Colquhoun, D., Burnstock, G. & Wood, J.N. (1995). “A P2X purinoreceptor expressed by a subset of sensory neurons”. *Nature*. **377**: 428-431.
- Cockayne, D.A., Hamilton, S.G., Zhu, Q., Dunn, P.M., Zhong, Y., Novakovic, S. et al. (2000). “Urinary bladder hyporeflexia and reduced pain-related behaviour in P2X3-deficient mice”. *Nature*. **407**: 1011-1015.
- Cockayne, D.A., Dunn, P.M., Zhong, Y., Rong, W., Hamilton, S.G., Knight, G.E. et al. (2005). “P2X2 knockout mice and P2X2/P2X3 double knockout mice reveal a role for the P2X2 receptor subunit in mediating multiple sensory effects of ATP”. *The Journal of Physiology*. **567** (2): 621-639.

- Decosterd, I. & Woolf, C.J. (2000). "Spared nerve injury: an animal model of persistent peripheral neuropathic pain". *Pain*. **87**: 149-158.
- Ding, S., Zhu, L., Tian, Y., Zhu, T., Huang, X. & Zhang, X. (2017). "P2X3 receptor involvement in endometriosis pain via ERK signaling pathway". *PLoS ONE*. **12** (9): e0184647.
- Dosch, M., Gerber, J., Jebbawi, F. & Beldi, G. (2018). "Mechanisms of ATP Release by Inflammatory Cells". *International Journal of Molecular Sciences*. **19** (4): e122.
- Eriksson, J., Bongenhielm, U., Kidd, E., Matthews, B. & Fried, K. (1998). "Distribution of P2X3 receptors in the rat trigeminal ganglion after inferior alveolar nerve injury". *Neuroscience Letters*. **254** (1): 37-40.
- Ford, A.P. (2012). "In pursuit of P2X3 antagonists: novel therapeutics for chronic pain and afferent sensitization". *Purinergic Signalling*. **8**: 3-26.
- Ford, A.P. & Udem, B.J. (2013). "The therapeutic promise of ATP antagonism at P2X3 receptors in respiratory and urological disorders". *Frontiers in Cellular Neuroscience*. **7** (267): doi:103389/fncel.2013.00267.
- Gever, J.R., Soto, R., Henningsen, R.A., Martin, R.S., Hackos, D.H., Panicker, S. et al. (2010). "AF-353, a novel, potent and orally bioavailable P2X3/P2X2/3 receptor antagonist". *British Journal of Pharmacology*. **160**: 1387-1398.
- Grishin, E.V., Savchenko, G.A., Vassilevski, A.A., Korolkova, Y.V., Boychuk, Y.A., Viatchenko-Karpinski, V.Y. et al. (2010). "Novel peptide from spider venom inhibits P2X3 receptors and inflammatory pain". *Annals of Neurology*. **67** (5): 680-683.
- Harding, SD, Sharman, JL, Faccenda, E, Southan, C, Pawson, AJ, Ireland, S et al. (2018). The IUPHAR/BPS Guide to PHARMACOLOGY in 2018: updates and expansion to encompass the new guide to IMMUNOPHARMACOLOGY. *Nucl Acids Res* **46**: D1091– D1106.
- Hilliges, M., Weidner, C., Schmelz, R., Schmidt, R., Orstavik, K., Torebjork, E et al. (2002). ATP responses in human C nociceptors. *Pain* **98**: 6704-12.
- Higenbottam, T (2002). "Chronic cough and the cough reflex in common lung disease". *Pulmonary Pharmacology & Therapeutics*. **15**: 241-247.
- Honore, P., Mikusa, J., Bianchi, B., McDonald, H., Cartmell, J., Faltynek, C. et al. (2002). "TNP-ATP, a potent P2X3 receptor antagonist blocks acetic acid-induced abdominal constriction in mice: comparison with reference analgesics". *Pain*. **96**: 99-105.
- Jarvis MF, Wismer CT, Schweitzer E, Yu H, van Biesen T, Lynch KJ, et al. Modulation of BzATP and formalin induced nociception: attenuation by the P2X receptor antagonist, TNP-ATP and enhancement by the P2X3 allosteric modulator, cibacron blue. *Br J Pharmacol*. 2001;132:259–269.

- Jarvis, M.F., Burgard, E.C., McGaraughty, S., Honore, P., Lynch, K., Brennan, T.J. et al. (2002). "A-317491, a novel potent and selective non-nucleotide antagonist of P2X3 and P2X2/3 receptors, reduces chronic inflammatory and neuropathic pain in the rat". *Proceedings of the National Academy of Sciences USA*. **99**:17179-17184.
- Kaan, T.K.Y., Yip, P.K., Patel, S., Davies, M., Marchand, D., Cockayne, D.A. et al. (2010). "Systemic blockade of P2X3 and P2X2/3 receptors attenuates bone cancer pain behaviour in rats". *Brain*. **133** (9): 2549-2564.
- Kawate, T., Michel, J.C., Birdsong, W.T. & Gouaux, E. (2009). "Crystal structure of the ATP-gated P2X4 channel in the closed state". *Nature*. **460** (7255): 592-598.
- Lewis, C., Neidhart, S., Holy, C., North, R.A., Buell, G. & Surprenant, A. (1995). "Co-expression of P2X2 and P2X3 receptor subunits can account for ATP-gated currents in sensory neurons". *Nature*. **377**: 432-435.
- Li, C. (2000). "Novel mechanism of inhibition by the P2 receptor antagonist PPADS of ATP-activated current in dorsal root ganglion neurons". *Journal of Neurophysiology*. **83** (5): 2533-2541.
- Mansoor, S.E., Lü, W., Oosterheert, W., Shekhar, M., Tajkhorshid, E. & Gouaux, E. (2016). "X-ray structures define human P2X(3) receptor gating cycle and antagonist action". *Nature*. **538**: 66-71.
- Mazzone, S.B. (2005). "An overview of the sensory receptors regulating cough". *Cough* **1**: 2.
- McGaraughty, S., Wismer, C.T., Zhu, C.Z., Mikusa, J., Honore, P., Chu, K.L. et al (2003). "Effects of A-317491, a novel and selective P2X3/P2X2/3 receptor antagonist, on neuropathic, inflammatory and chemogenic nociception following intrathecal and intraplantar administration". *British Journal of Pharmacology*. **140** (8): 1381-1388.
- North, R.A. (2002). Molecular physiology of P2X receptors. *Physiological Reviews*. **82**: 1013-67.
- North, R.A. (2004). P2X3 receptors and peripheral pain mechanisms. *Journal of Physiology*. **554**: 301-308.
- Novakovic, S.D., Kassotakislan, L.C., Oglesby, I.B., Smith J.A.M., Eglen, R.M., Ford, A.P.D.W. et al. (1999). "Immunocytochemical localization of P2X3 purinoreceptors in sensory neurons in naïve rats and following neuropathic injury". *Pain*. **80** (1-2): 273-282.
- Pijacka, W., Moraes, D.J., Ratcliffe, L.E., Nightingale, A.K., Hart, E.C., da Silva, M.P. et al (2016). "Purinergeric receptors in the carotid body as a new drug target for controlling hypertension". *Nature Medicine*. **22** (10): 1151-1159.
- Sekino, Y., Nakano, J., Hamaue, Y., Chuganji, S., Sakamoto, J., Yoshimura, T. et al. (2014). "Sensory hyperinnervation and increase in NGF, TRPV1 and P2X3 expression in the epidermis following cast immobilization in rats". *European Journal of Pain*. **18** (5): 639-648.

- Shcherbatko, A., Foletti, D., Poulsen, K., Strop, P., Zhu, G., HasaMoreno, A. et al. (2016). "Modulation of P2X3 and P2X2/3 receptors by monoclonal antibodies". *Journal of Biological Chemistry*. **291** (23): 12254-12270.
- Shinoda, M., Ozaki, N., Asai, H., Nagamine, K. & Sugiura, Y. (2005). "Changes in P2X3 receptor expression in the trigeminal ganglion following monoarthritis of the temporomandibular joint in rats". *Pain*. **116** (1-2): 42-51.
- Spelta, V., Jiang, L., Surprenant, A. & North, A. (2002). "Kinetics of antagonist actions at rat P2X2/3 heteromeric receptors". *British Journal of Pharmacology*. **135**: 1524-1530.
- Stein, C., Millan, M.J. & Herz, A. (1988). "Unilateral inflammation of the hindpaw in rats as a model of prolonged noxious stimulation: Alterations in behaviour and nociceptive thresholds". *Pharmacology Biochemistry and Behavior*. **31** (2): 445-451.
- Stokes, L., Layhadi, J.A., Bibic, L., Dhuna, K. & Fountain, S.J. (2017). P2X4 receptor function in the central nervous system and current breakthroughs in pharmacology. *Front Pharmacol*. **23**: 291.
- Surprenant, A. & North, R.A. (2009). "Signaling at purinergic P2X receptors". *Annual Review of Physiology*. **71**: 333-359.
- Tempest, H.V., Dixon, A.K., Turner, W.H., Elneil, S., Sellers, L.A. & Ferguson, D.R. (2004). "P2X2 and P2X3 receptor expression in human bladder urothelium and changes in interstitial cystitis". *British Journal of Urology International*. **93** (9): 1344-1348.
- Teixeira, J.M., Bobinski, F., Parada, C.A., Sluka, K.A. & Tambeli, C.H. (2017). P2X3 and P2X2/3 receptors play a crucial role in articular hyperalgesia development through inflammatory mechanisms in the knee joint experimental synovitis. *Mol Neurobiol*. **54**: 6174-6186.
- Ueno S, Moriyama T, Honda K, Kamiya H, Sakurada T, Katsuragi T. Involvement of P2X₂ and P2X₃ receptors in neuropathic pain in a mouse model of chronic constriction injury. *Drug Dev Res*. 2003;59:104-111.
- Wang, J., Wang, Y., Cui, W., Huang, Y., Yang, Y., Liu, Y. et al. (2018). "Druggable negative allosteric site of P2X3 receptors". *Proceedings of the National Academy of Science*. **115** (19): 4939-4944.
- Zhong, Y., Dunn, P.M., Bardini, M., Ford, A.P.D.W., Cockayne, D.A. & Burnstock, G. (2001). "Changes in P2X receptors responses of sensory neurons from P2X3-deficient mice". *European Journal of Neuroscience*. **14** (11): 1784-1792.
- Xiang, Z., Bo, X. & Burnstock, G. (1998). "Localization of ATP-gated P2X receptor immunoreactivity in rat sensory and sympathetic ganglia". *Neuroscience Letters*. **256** (2): 105-108.

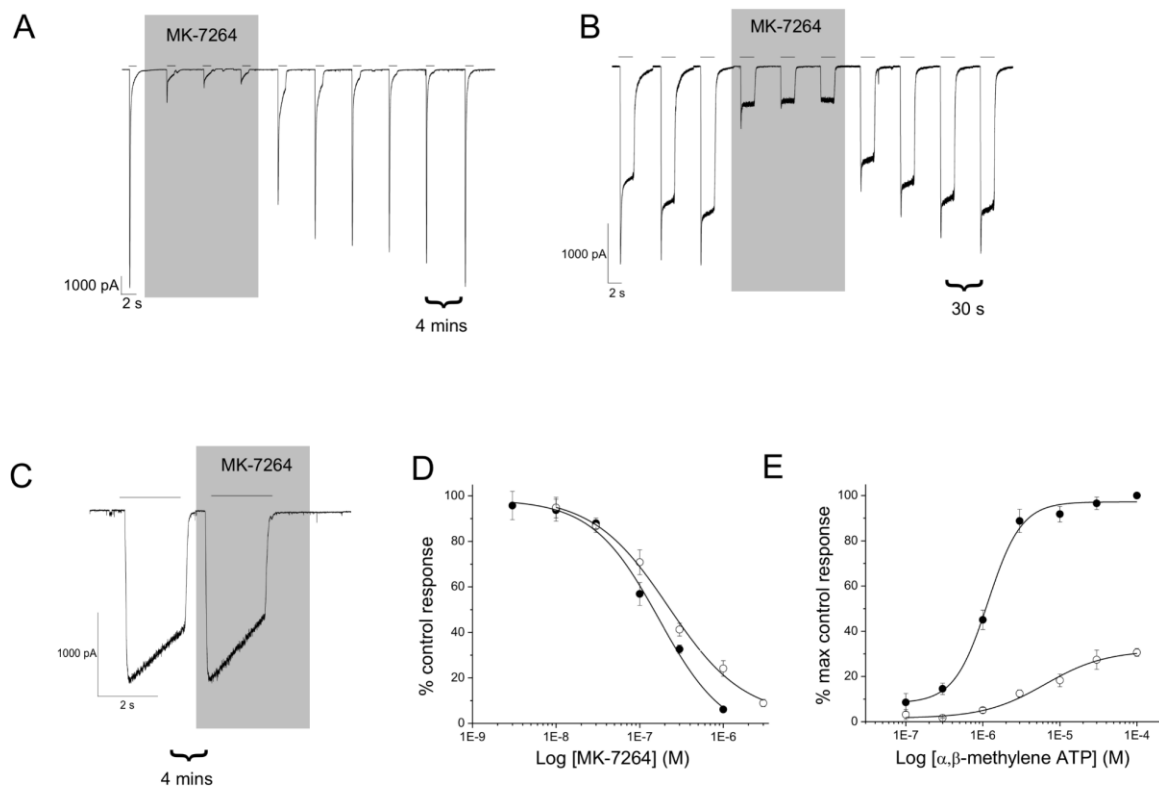


Figure 1

Figure 1 MK-7264 activity at human P2X2, P2X3 and P2X2/3 receptors. (A-C) shows representative concatenated traces of whole-cell patch-clamp recordings for human P2X3 (A), P2X2/3 (B) and P2X2 (C) receptor currents in 1312N1 stably transfected cells. Fully recovered P2X3 currents are evoked by 10 μM α,β-meATP applied for 1 s every 4 mins, and 10 μM α,β-meATP applied for 2 s at 30 s intervals for P2X2/3 currents. P2X2 currents are evoked by 10 μM ATP every 4 mins. MK-7264 was applied 4 mins, 30 s and 4 mins prior to agonist application for P2X3 (1 μM), P2X2/3 (1 μM) and P2X2 (10 μM) receptors, respectively. Agonist application is indicated by the perfusion bar. Currents shaded in grey are in the presence of MK-7264. (D) MK-7264 concentration-inhibition curve at human P2X3 (*closed circles*) and P2X2/3 receptors (*open circles*) ($N=5$). Data sets were compared with an F-test and found to be significantly different from one another ($F = 11.74$, $P = 0.018$) (E) Effect of MK-7264 on α,β-meATP concentration-response curve at P2X3. Currents are in the presence of 300 nM MK-7264 (*open circles*) or vehicle control (*closed circles*) ($N=6$). MK-7264 applied for 4 mins prior to agonist application. EC_{50} values were compared with a paired-sample T-test and found to be significantly different ($P = 0.018$). The holding potential was -80 mV for all experiments.

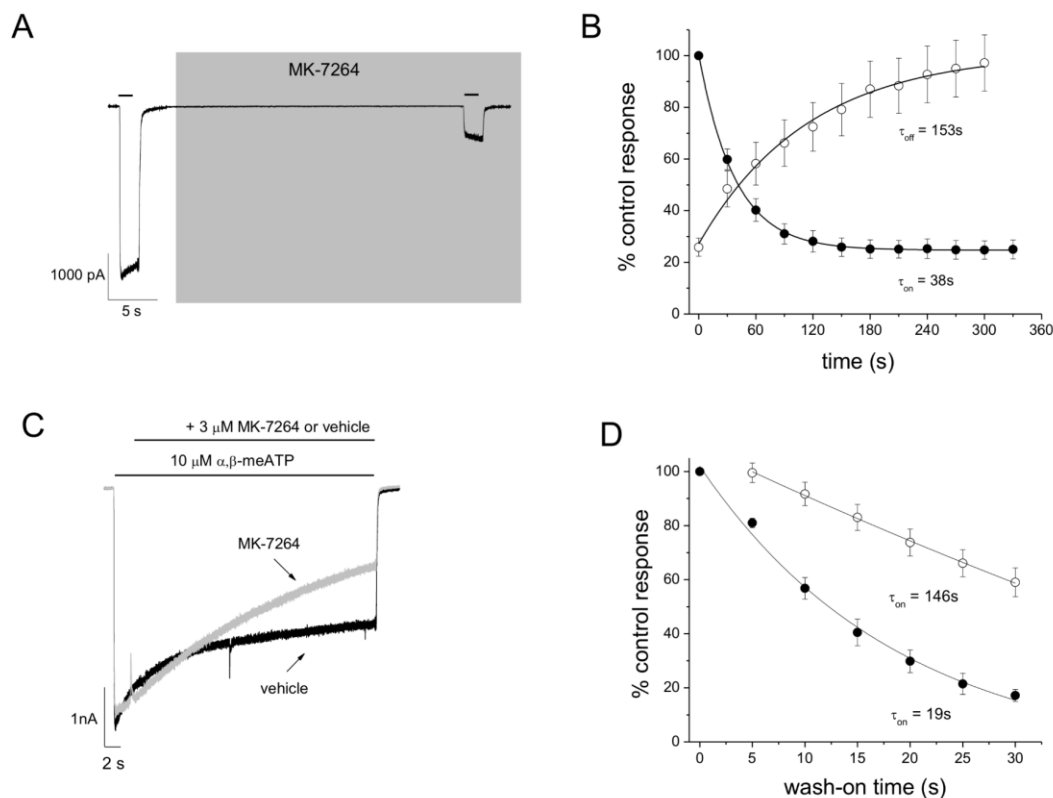


Figure 2

Figure 2 MK-7264 antagonism has different on-rates when applied before or during agonist application at the human P2X2/3 receptor. (A) Representative trace showing effect of a 30 s preincubation with 3 μ M MK-7264 on currents evoked by 10 μ M α,β -meATP at human P2X2/3 receptors. Agonist application is indicated by the perfusion bar. Currents shaded in grey are in the presence of MK-7264. (B) The effect of varying preincubation time of MK-7264 (3 μ M) on antagonism of P2X2/3 responses (10 μ M α,β -meATP, 2s) (*closed circles*; $N=7$), and the effect of wash-off time on response recovery following maximal antagonism (*open circles*). Time constants (τ values) are calculated from single exponential curve fits. Data is normalised to the control response prior to MK-7264 application. (C) Representative trace showing effect of rapid co-application of agonist and MK-7264. Responses were evoked with 10 μ M α,β -meATP for 2s followed by co-application with 3 μ M MK-7264 or vehicle. (D) Relationship between magnitude of P2X2/3 antagonism and wash on time during α,β -meATP application (*open circles*) and before application (*closed circles*). Data is normalised to response prior to MK-7264 application (*closed circles*) or the magnitude of response at the same time point in the presence of vehicle (*open circles*) ($N=5$). Datasets were compared with a One-way ANOVA ($F = 45.95$, $P < 0.05$) followed by Tukey post hoc test.

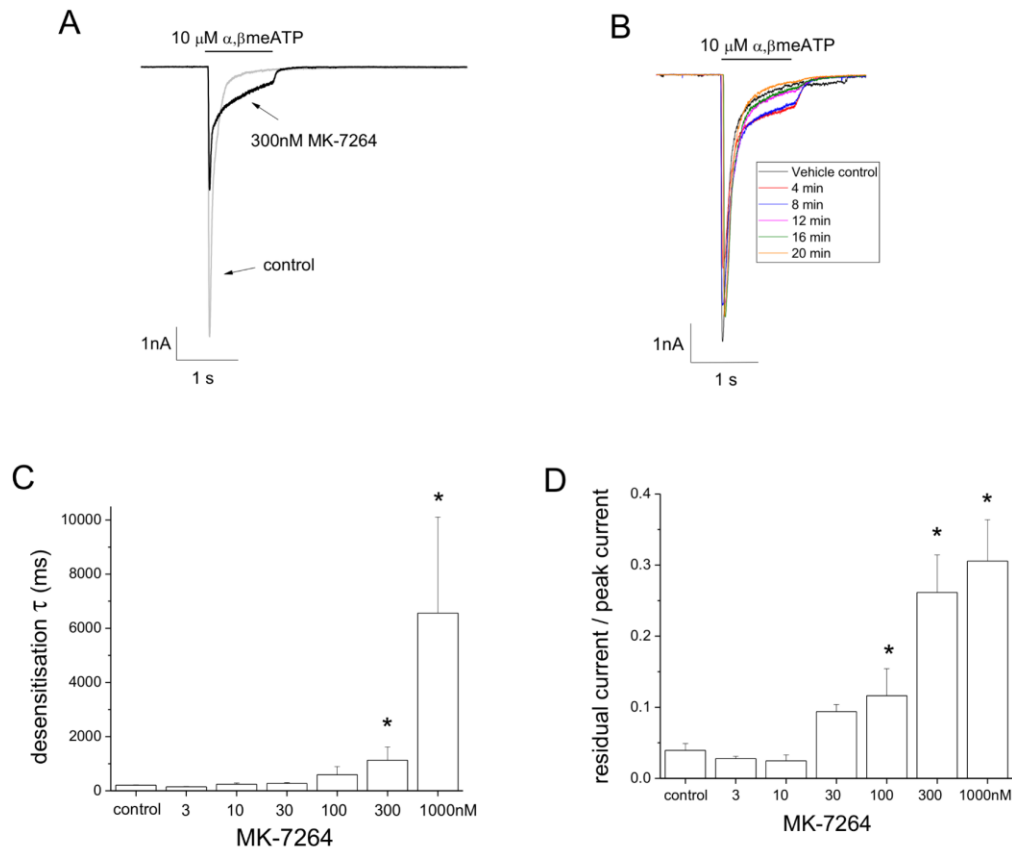


Figure 3

Figure 3 MK-7264 antagonism of human P2X3 receptor is associated with an onset of slowed desensitisation. (A) Representative trace showing a diminished peak response and appearance of slow desensitisation are associated with MK-7264 antagonism. (B) Representative superimposed trace showing time-dependent recovery of P2X3 fast desensitisation following MK-7264 (300nM) wash-off. Agonist applied every 4 mins. (C) Relationship between MK-7264 concentration and the rate of desensitisation. Time constants (τ values) are derived from single exponential curves fitted to the desensitisation phase 250-750ms after the peak response. Tau values were compared with a Kruskal-Wallis ANOVA ($P < 0.0001$) followed by Dunn's post hoc test $N=6$. (D) The change in shape of the current following MK-7264 antagonism quantified as a fractional response (residual current, 1s after onset of agonist response over peak current) and compared with a Kruskal-Wallis ANOVA followed by Dunn's post hoc test. * $P < 0.05$ versus control response; $N=7$.

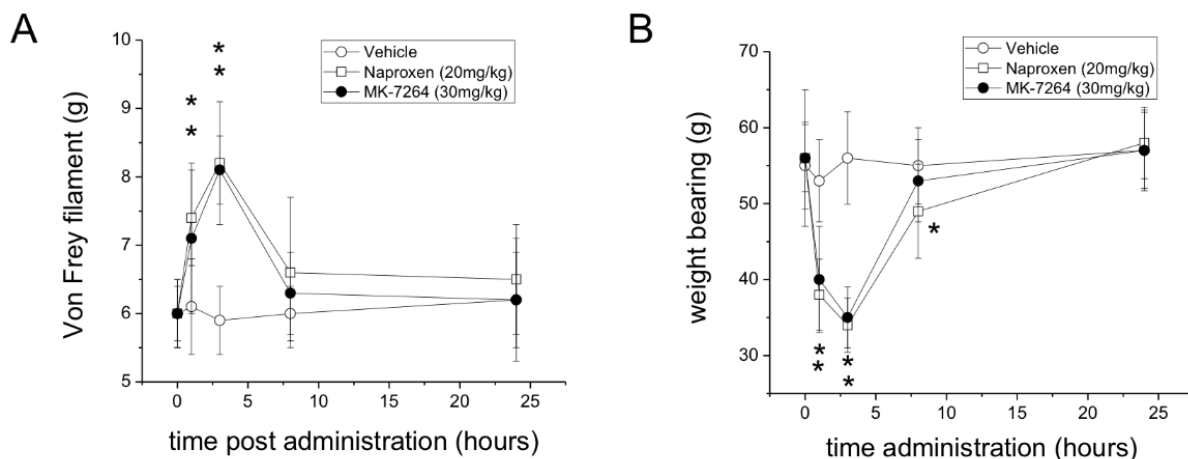


Figure 4 MK-7264 efficacy in a rat model of inflammatory hyperalgesia. Complete Freund's adjuvant hindpaw injection model of inflammatory hyperalgesia. (A) Effect of single oral dose of vehicle, naproxen or MK-7264 on paw withdrawal threshold determined by Von Frey filament testing ($N=10$). (B) Effect of single oral dose of vehicle, naproxen or MK-7264 on postural equilibrium (weight bearing) of inflamed versus non-inflamed hindlimb ($N=10$). Naproxen serves as a positive control. Sodium carboxymethyl cellulose is the vehicle control. Drug treatments were compared with a Two-way repeated measures ANOVA followed by Fisher least significant difference post hoc test. * $P<0.05$ versus vehicle control.

Accepted

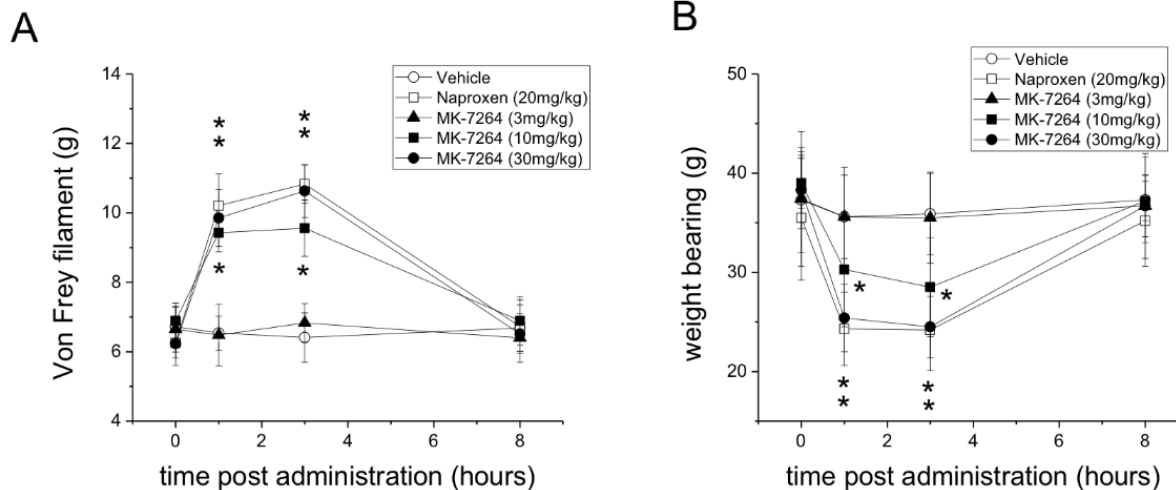


Figure 5 MK-7264 efficacy in a rat model of osteoarthritic pain. Mono-iodoacetate (MIA) hind knee injection model of osteoarthritic pain. (A) Effect of single oral dose of vehicle and naproxen and ranging MK-7264 doses on paw withdrawal threshold determined by Von Frey filament testing ($N=10$). (B) Effect of single oral dose of vehicle and naproxen or ranging MK-7264 doses on postural equilibrium (weight bearing) of injected versus non-injected hindlimb ($N=10$). Drugs were administered 13 days following MIA injection. Naproxen serves as a positive control. Sodium carboxymethyl cellulose is the vehicle control. Drug treatments were compared with a Two-way repeated measures ANOVA followed by Fisher least significant difference post hoc test. * $P < 0.05$ versus vehicle control.

Accepted

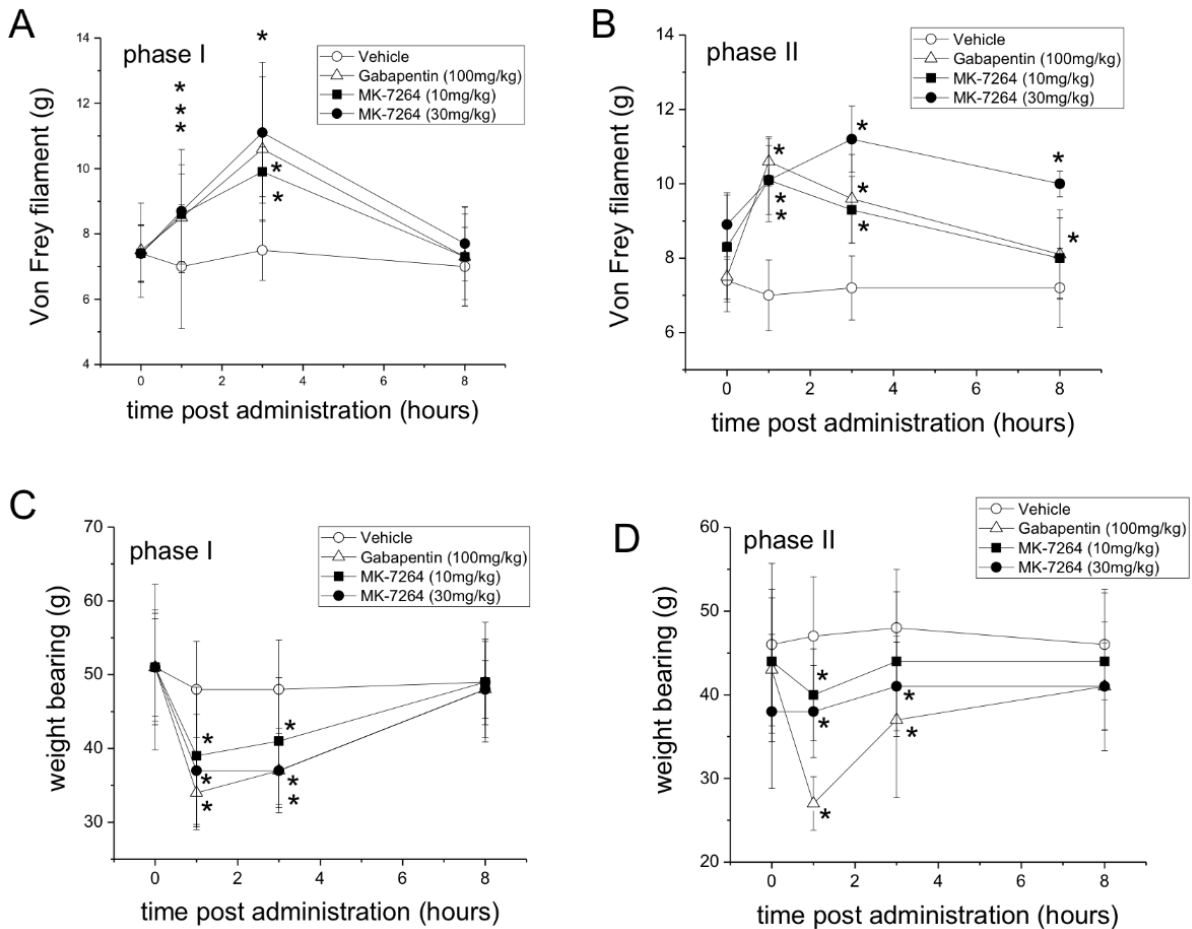


Figure 6 MK-7264 efficacy in a rat spared nerve model of neuropathic pain. Sciatic nerve injury model induced by axotomy of peroneal and tibial nerves. Phase I experiments represent single oral dosing 10 days after surgery. Following completion of the Phase I dosing regimen, Phase II experiments were undertaken using oral dosing every 12 hours for 5.5 days to test for drug tolerance. (A and B) Effect of phase I dosing (A) and phase II dosing (B) regimens on paw withdrawal threshold determined by Von Frey filament testing ($N=10$). (C and D) Effect of phase I dosing (C) and phase II dosing (D) regimens on postural equilibrium (weight bearing) of injected versus non-injected hindlimb ($N=10$). Gabapentin serves as a positive control. Sodium carboxymethyl cellulose is the vehicle control. Drug treatments were compared with a Two-way repeated measures ANOVA followed by Fisher least significant difference post hoc test. * $P<0.05$ versus vehicle control.

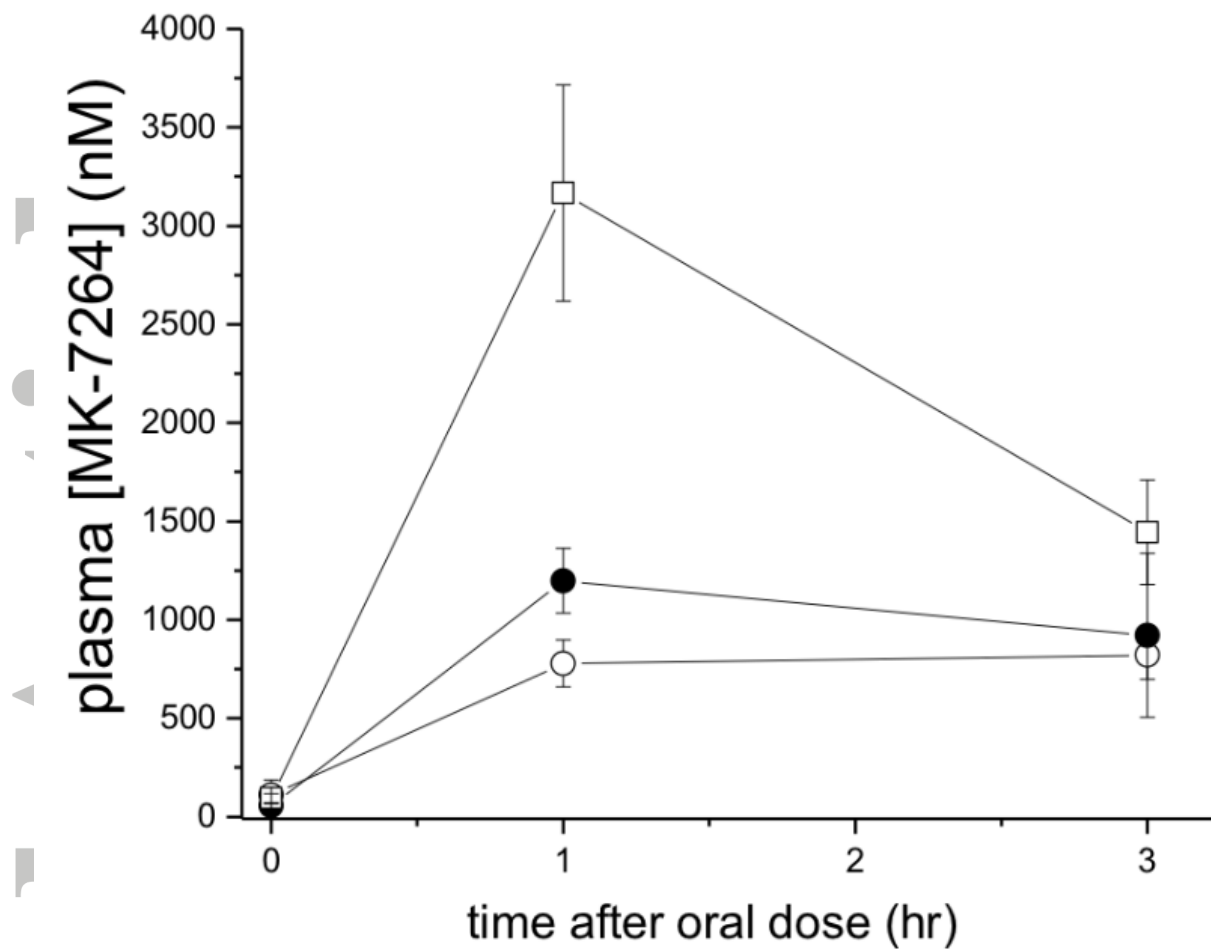


Figure 7 Plasma concentration of MK-7264 following oral dosing in rats. Quantification of MK-7264 plasma concentration following oral dosing with 10 (*open circles*), 20 (*closed circles*) and 60 (*squares*) mg/kg at 0, 1 and 3 hours after dosing ($N=5$). Sampling from orbital blood.

Accepted

Table 1 Mean τ_{on} and τ_{off} times for MK-7264 at the human P2X_{2/3} receptor. Rates were estimated by fitting a single exponential decay to individual data sets for mean 1-2 second current during onset and offset of antagonist effect. Data shown is the mean \pm SEM of 6 cells. Cells were held at -80 mV.

MK-7264 concentration (nM)	Mean $\tau_{\text{on}} \pm$ SEM (s)	Mean $\tau_{\text{off}} \pm$ SEM (s)
3000	11.82 (\pm 0.66)	113.43 (\pm 14.42)
1000	38.04 (\pm 2.34)	152.95 (\pm 14.12)
300	176.04 (\pm 27.59)	183.04 (\pm 24.14)
100	359.78 (\pm 141.98)	258.11 (\pm 45.96)

Accepted Article